Biosensors and Bioelectronics 68 (2015) 168–174

Contents lists available at ScienceDirect

Biosensors and Bioelectronics

journal homepage: www.elsevier.com/locate/bios

Upconversion nanoparticle-based fluorescence resonance energy transfer assay for organophosphorus pesticides

Qian Long, Haitao Li, Youyu Zhang *, Shouzhuo Yao

Key Laboratory of Chemical Biology and Traditional Chinese Medicine Research (Ministry of Education), College of Chemistry and Chemical Engineering, Hunan Normal University, Changsha 410081, PR China

ARTICLE INFO

Article history:
Received 27 September 2014
Received in revised form
18 December 2014
Accepted 20 December 2014
Available online 23 December 2014

Keywords:
Upconversion nanoparticles
Gold nanoparticle
Fluorescence resonance energy transfer
Organophosphorus pesticides

ABSTRACT

This paper reports a novel nanosensor for organophosphorus pesticides based on the fluorescence resonance energy transfer (FRET) between $NaYF_4$:Yb,Er upconversion nanoparticles (UCNPs) and gold nanoparticles (AuNPs). The detection mechanism is based on the facts that AuNPs quench the fluorescence of UCNPs and organophosphorus pesticides (OPs) inhibit the activity of acetylcholinesterase (AChE) which catalyzes the hydrolysis of acetylthiocholine (ATC) into thiocholine. Under the optimized conditions, the logarithm of the pesticides concentration was proportional to the inhibition efficiency. The detection limits of parathion-methyl, monocrotophos and dimethoate reached 0.67, 23, and 67 ng/L, respectively. Meanwhile, the biosensor shows good sensitivity, stability, and could be successfully applied to detection of OPs in real food samples, suggesting the biosensor has potentially extensive application clinic diagnoses assays.

1. Introduction

Organophosphorus pesticides (OPs) are widely used in agriculture due to their relatively low persistence under natural conditions, easy synthesis, low cost and high effectiveness for insect eradication, which comes to ensure the high production of crops (Zheng et al., 2011a, 2011b; Liu et al., 2012; Li et al., 2014). However, the wide use of pesticides have resulted in the widespread contamination of water, atmosphere, soil and agricultural products (Yi et al., 2013) and eventually lead to food safety issues (Liu et al., 2012; Guo et al., 2013). The most widely-used insecticides exhibited acute toxicity on human health even at very low levels. According to the World Health Organization, 1.5 billion cases of diarrhea in children (leading to more than 3 million deaths) are caused by contaminated food each year (Yi et al., 2013). The high toxicity of organophosphorus pesticides is attributed to the their ability to irreversibly inhibit the activity of acetylcholinesterase (AChE) (Liu et al., 2012). AChE is a key enzyme in the central and peripheral nervous system, which possesses extraordinarily high catalytic activity to break down the acetylcholine (a neurotransmitter) at cholinergic synapses through rapid hydrolysis of acetylcholine into choline and acetate (Jia et al., 2013; Liao et al., 2013; Yi et al., 2013). Organophosphorus pesticides inhibit the activity of acetylcholinesterase (AChE) and allow acetylcholine to remain active in the synapse which can lead to deadly consequences such as cause muscarinic, nicotinic and central nervous system symptoms, and even coma and respiratory failure and death for severe patients (Yi et al., 2013). Therefore, development of an efficient, reliable assay and simple method for monitoring and quantifying organophosphorus pesticides in complex samples is important to improve food safety.

In the past decade, great effort has been made to develop various efficient methods to determine pesticides in food or water. Among the numerous analytical methods, electrochemical analysis (Liu and Lin, 2005; Viswanathan et al., 2009; Chauhan and Pundir, 2011; Du et al., 2011; Tian et al., 2011; Yong et al., 2011; Yang et al., 2014), liquid/gas chromatography-mass spectrometry (Payá et al., 2007; Buonasera et al., 2009; Lee and Lee, 2011; Seebunrueng et al., 2014; Zhu et al., 2014), enzyme-linked immunosorbent assays (ELISAs) (Gabaldón et al., 2007; Qian et al., 2009; Jiang et al., 2011), colorimetric assay (Liang et al., 2012; Liu et al., 2012; Fu et al., 2013) and fluorescence assay (Peng et al., 2009; Zhang et al., 2010; Zhao et al., 2011; Zheng et al., 2011a, 2011b; Guo et al., 2013; Yi et al., 2013) are widely used. Although these methods mentioned above are of high selectivity and sensitivity, many of them involved laborious synthetic procedures, tedious pretreatment of samples, time-consume immobilizing processes and sophisticated instrumentation. Optical methods, especially fluorescence methods, have many advantages such as reliable, simple instruments, easiness for operation and high sensitivity. But they are still limited because of the difficulty to eliminate the background interference in complex sample matrices. Therefore, it is imperative to

* Corresponding author. Fax: +86 731 88865515.
E-mail address: zhangyy@hunnu.edu.cn (Y. Zhang).

http://dx.doi.org/10.1016/j.bios.2014.12.046
0956-5663/

develop simple, highly sensitive and inexpensive fluorescence methods for the rapid detection of pesticides without autofluorescence interference and photobleaching.

In recent years, lanthanide-doped near-infrared (NIR)-to-visible upconversion nanoparticles (UCNPs) are capable of emitting strong visible luminescence with the excitation of NIR light (typically 980 nm) (Wu et al., 2014) via a two-photon or multiphoton mechanism (Chen et al., 2013a, 2013b; Ma et al., 2014). Compared with the traditional organic fluorophores, UCNPs as fluorescent biolabels, possess several unique qualities, such as attractive optical and chemical features, low cytotoxicity, large Stokes shifts, greater tissue penetration, long lifetimes, high resistance to photobleaching, blinking and photochemical degradation (Liu et al., 2011; Chen et al., 2013a, 2013b; Liu et al., 2013; Zhou et al., 2014). More importantly, compared with organic fluorophores and QDs, the excitation light of UCNPs (NIR light) can not be absorbed by biological samples (Liu et al., 2011), which could eliminate the autofluorescence by biological samples, thus providing an enlarged signal-to-background ratio and improved sensitivities (Liu et al., 2011; Wang et al., 2012; Li and Wang 2013; Liu et al. 2013; Zhou et al., 2014). To the best of our knowledge, there is no study associated with enzyme-catalyzed events by using UCNPs. Therefore, the development of new method by using UCNPs has great significance in investigation of complicated enzyme-catalyzed system.

In this work, we designed a new UC-FRET-based optical biosensor by means of an assembly of UCNPs and AuNPs for the detection of organophosphorus pesticides. The proposed novel strategy for pesticide detection is shown in Scheme 1. An efficient fluorescence resonance energy transfer (FRET) would occur between UCNPs and AuNPs, with UCNPs acting as the donors and AuNPs as the acceptors. The fluorescence of UCNPs can be significantly quenched by AuNPs attached to the surface of UCNPs through electrostatic interaction. Acetylthiocholine (ATC) is an analog of acetylcholine, a substrate of AChE, and it can be easily hydrolyzed to generate thiocholine. The electrostatic interactions and gold–thiols interaction between thiocholine and AuNPs resulted the disintegration of the AuNPs/UCNPs assembly and the aggregation of AuNPs. In the presence of pesticides, the activity of AChE is inhibited by pesticides, which preventing the generation of thiocholine and the FRET system formed, thus the fluorescence of UCNPs is quenched.

2. Experimental sections

2.1. Materials and apparatus

Rare earth oxides, including Y_2O_3, Yb_2O_3, Er_2O_3, were purchased from China National Pharmaceutical Group Corporation (Shanghai, China). acetylcholinesterase (AChE) (from electrophorus electricus) and Acetylthiocholine (ATC) were obtained from Sigma-Aldrich (Shanghai, China). Dimethoate, monocrotophos and parathion-methyl were from Huaerbo Chemical Reagent Co. NaCl, KCl, $FeCl_3$, $MgCl_2$, $AlCl_3$, $CaCl_2$, Na_2SO_4, Na_2CO_3, $ZnCl_2$, Na_3PO_4, $NaHCO_3$, $GdCl_2$, glucose, fructose, 2-nitrophenol, proline, histidine, arginine and vitamin C were purchased from Beijing Chemical Corp. All the other chemicals (99%, Merck) used in this work were of analytical grade and Millipore Milli-Q ultrapure water was used throughout the experiments. The UV-245 spectrophotometer (Shimadzu Co., Japan) was used to collect the absorption spectra of AuNPs. The fluorescent emission spectra of UCNPs were recorded by the F-4500 fluorescence spectrophotometer (Hitachi Co., Japan). Transmission electron microscopy (TEM) images were collected by the JEOL-1230 transmission electron microscope (JEM-3010 Joel, Japan). The ζ potential measurement was performed by the Nano-ZS Zetzsozer ZEN3600 (Malvern Instruments Ltd., UK). High-performance liquid chromatography (HPLC; Agilent 1200, USA) analysis was performed on a Zorbax SB-C18 column (150 mm × 4.6 mm i.d., 4 μm).

2.2. Experimental procedure for the fluorescence detection of pesticides

Various amounts of pesticides were added to same AChE solution (10 mU/mL), which were then kept in the dark for 30 min. UCNPs (30 μL, 0.06 mg mL^{-1}), AuNPs (0.2 mL, 1.28 nM), PBS (10 mM, pH=8.0) were then added into each mixture and finally aliquots of ATC (10 μM) were added into the mixtures. The resulting mixtures were kept in the dark for 20 min (the final volume is 500 μL), and the fluorescence emission spectra were measured with excitation wavelength at 980 nm. The relationships between the percentage enzyme inhibition and the concentrations of pesticides were plotted into calibration curves.

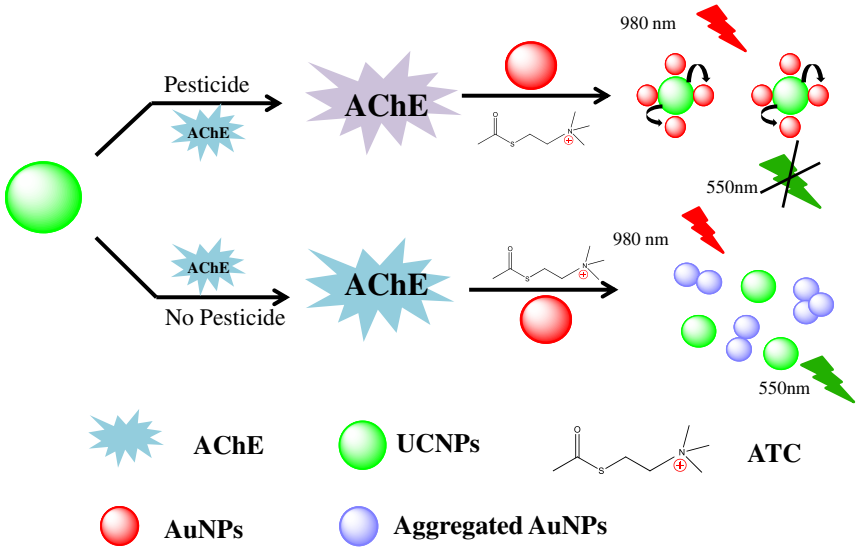

Scheme 1. Schematic illustration of the UCNPs–AuNPs fluorescence assay for the detection of pesticides.

3. Results and discussion

3.1. Characteristics of UCNPs and AuNPs

The morphology, structure and optical properties of UCNPs were characterized by TEM, XRD, FTIR and fluorescence spectra, and the results are shown in Figs. 1 and S1–3. The TEM results (Fig. 1A) suggested that the as-prepared UCNPs are spherical in shape and fairly uniform in size (average size: 30 nm). The typical XRD patterns of the as-prepared UCNPs are presented in Fig. S1. The peak positions are in good agreement with the standard values for cubic (JCPDS no. 77-2042), indicating the highly crystalline nature possessed the synthesized material. As shown in Fig. S2 (curve 2), two strong absorption bands at 2934 cm^{-1} and 2865 cm^{-1} are assigned to the C–H ($-CH_3$ and $-CH_2-$) stretch and a weak absorption near 1480 cm^{-1} is attributed to the symmetric deformation mode of the amine group, which were consistent with pure CTAB, seen Fig. S2 (curve 1). Due to CTAB capped onto the surface of UCNPs, the UCNPs could be well-dispersed in water and could directly form a colloidal solution without any surface modification. At the same time, UCNPs are very stable in the aqueous solution and the fluorescence intensity remained unchanged within 60 min as shown in Fig. S3A. Upon further investigation, we found that the fluorescence intensity of UCNPs was not affected by pH (Fig. S3B). Fig. 1C (curve 1) represen the fluorescence spectra of UCNPs upon excitation with a 980 nm laser, and three characteristic peaks at 530, 550, and 665 nm were observed, which were assigned to transitions from the $^2H_{11/2}$, $^4S_{3/2}$, and $^4F_{9/2}$ excited states to the $^4I_{15/2}$ ground state, respectively (Chen et al., 2013a, 2013b).

AuNPs were also characterized by TEM and UV–vis spectroscopy and the results were shown in Fig. 1. It can be seen that the as-prepared AuNPs are spherical in shape, highly monodisperse and fairly uniform in size (average size: 25 nm) (Fig. 1B). Fig. 1C (curve 2) showed the absorption spectrum of AuNPs. AuNPs have a characteristic surface plasmon resonance (SPR) peak located at 526 nm.

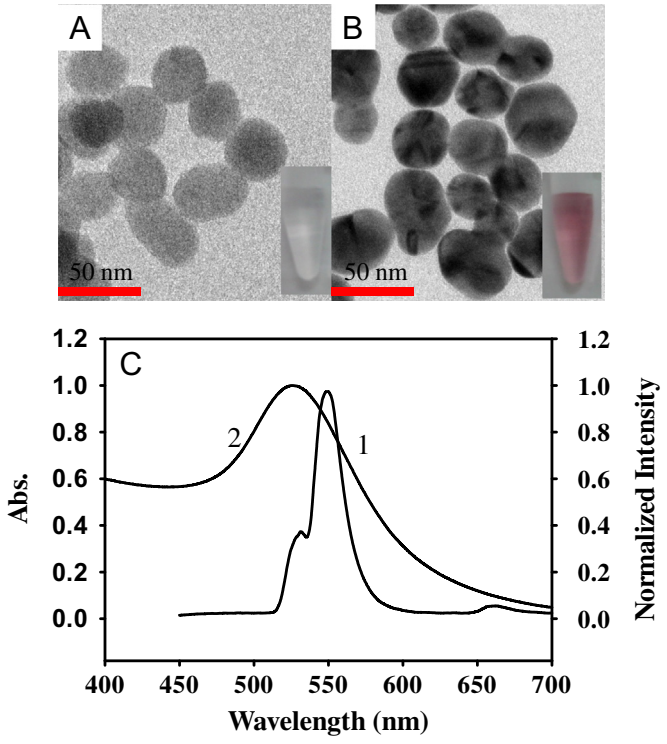

Fig. 1. TEM images of $NaYF_4$:Yb,Er UCNPs (A) and free AuNPs (B). (C) Emission spectrum of $NaYF_4$:Yb,Er UCNPs (1) and absorption spectrum of AuNPs (2).

3.2. FRET between UCNPs and AuNPs

AuNPs were prepared by the citrate reduction method in this work (Ji et al., 2007) which is stabilized against aggregation due to the negative capping agent's electrostatic repulsion against van der Waals attraction between AuNPs in aqueous solution (Chen et al., 2013a, 2013b). UCNPs carried with positive charge because the CTAB surfactant formed a positively charged layer on the surface of UCNPs (Chen et al., 2013a, 2013b). The zeta potential of AuNPs and UCNPs were presented in Fig. S4. The experimental results showed the zeta potentials of dispersed AuNPs and the CTAB-stabilized UCNPs were −19.8 mV and +23.1 mV, respectively. Therefore, the negatively charged AuNPs and the positively charged UCNPs can interact through electrostatic force. Fig. 1C shows the absorption spectrum of AuNPs and emission spectra of UCNPs. The maximum emission peak of UCNPs was located at 550 nm (curve 1). The characteristic surface plasmon resonance (SPR) peak of AuNPs (curve 2) was located at 526 nm. The absorption spectrum of AuNPs largely overlapped the emission spectrum of UCNPs, which indicted that efficient FRET between UCNPs and AuNPs occurred. We investigated the influence of the concentration of AuNPs on the FRET efficiency. As shown in Fig. S5A, with the increasing in the concentration of AuNPs (acceptor), the emission intensity of UCNPs (donor) decreases gradually. The data were analyzed by using the Stern–Volmer equation (Zhao et al., 2013)

$$I_0/I = Ksv \times [Q] + 1 \quad (1)$$

I_0 and I are the fluorescent intensity of UCNPs in the absence and presence of AuNPs, respectively. [Q] is the concentration of AuNPs and the unit is nM. The relationship between I_0/I and the concentration of AuNPs was shown in Fig. S5B. According to the Stern–Volmer quenching plot

$$I_0/I = 2.4 \times [Q] + 1 (R^2 = 0.96) \quad (2)$$

The quenching constant (Ksv) was estimated to be $2.4 \times 10^9\ M^{-1}$. This large quenching constant suggested that AuNPs could efficiently quench the fluorescence of UCNPs.

3.3. Detection strategy of pesticides

The basic principle of the UCNPs-based pesticide sensor includes the hydrolysis of ATC catalyzed by AChE, the inhibition of enzyme activity by pesticides and the fluorescent quenching of UCNPs by the AuNPs. Primarily, as shown in Fig. 2D, UCNPs solution exhibits a maximum fluorescent signal at 550 nm (curve 1). Compared to other signal source, UCNPs has been broadly applied in biosensor due to its high photoluminescence intensity, narrow emission band, good chemical stability, low damage to analytes and photostability. The UCNPs-based biosensor can eliminate the autofluorescence from biological macromolecules due to its visible emission under low-energy NIR excitation (normally 980 nm), which provides an enlarged signal-to-background ratio and increased sensitivities. The fluorescence emission of UCNPs can be effectively quenched by AuNPs when UCNPs was mixed with AuNPs through the FRET (curve 4). Secondly, AuNPs adsorbed on the surface of UCNPs can be released by introducing ATC and AChE. AChE catalyze the hydrolysis of ATC into thiocholine which can induce the aggregation of AuNPs and thus resulting in the recovery of fluorescence of UCNPs (curve 2). Ultimately, when the parathion-methyl was added to the sensing system, the activity of AChE was inhibited and then prevent the generation of thiocholine. The fluorescence recovery degree of the FRET system was decreased (curve 3). These phenomena are attributed to the fact that parathion-methyl is capable of inhibiting AChE activity, thus

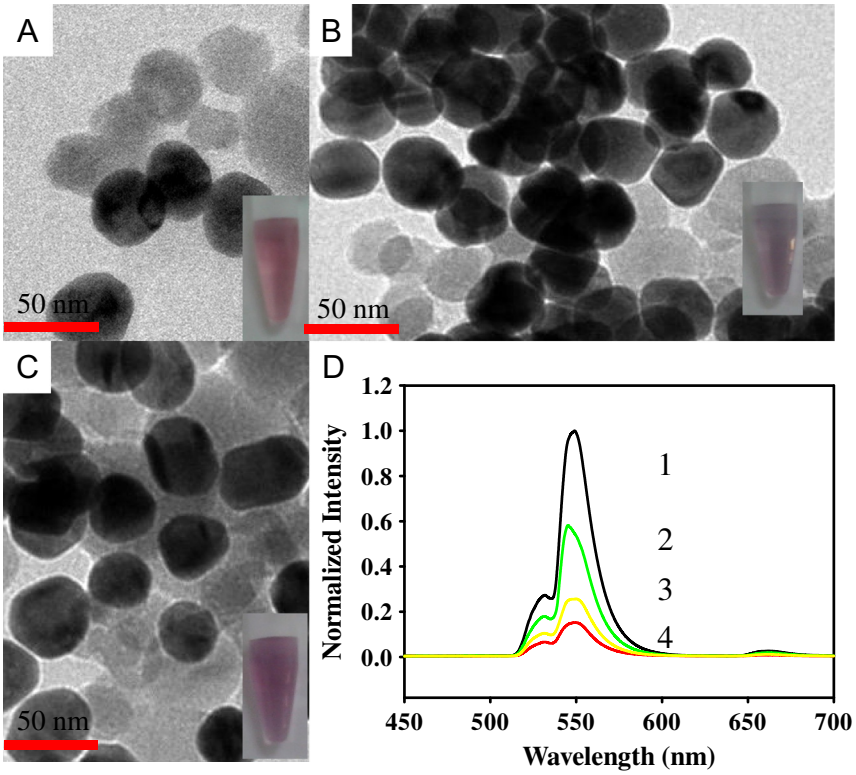

Fig. 2. TEM images of UCNPs in the presence of AuNPs (A), UCNPs–AuNPs after adding AChE and ATC (B) and UCNPs–AuNPs by pretreating AChE with parathion-methyl (C). (D) Fluorescence spectra of $NaYF_4$:Yb,Er UCNPs (1), UCNPs and AuNPs (4), the mixture of UCNPs–AuNPs AChE and ATC (2) and UCNPs–AuNPs incubated with parathion-methyl (3). [UCNPs]: 0.06 mg/mL, [AuNPs]: 1.28 nmol/L, [parathion-methyl]: 2.0×10^{-7} g/L. (For interpretation of the references to color in this figure the reader is referred to the web version of this article.)

preventing the generation of thiolcholine arising from the AChE-catalyzed hydrolysis of ATC (Liang et al., 2012; Yi et al., 2013). In order to evaluate the feasibility of this assay for parathion-methyl, we investigated the effects of the related factors. As shown in Fig. S6, the label-free UCNPs were individually incubated with AChE, ATC or parathion-methyl under the same condition, it is observed that there was almost no change and the fluorescent intensity was identical to that of UCNPs. In addition, the fluorescent spectrum of UCNPs–AuNPs has no significant change when UCNPs–AuNPs mixture individually incubated with AChE, ATC or parathion-methyl under the same conditions. The results indicated that the factors mentioned above should not affect the experimental results. The TEM images of UCNPs and the color changes of the test solution were also recorded at different stages, which proved the interaction among UCNPs, parathion-methyl, ATC, AChE and AuNPs (Fig. 2). As shown in Fig. 2A, AuNPs were retained in a dispersed state and the solution kept the red color in the presence of UCNPs. Fig. 2B shows a rapid red-to-blue color change of the solution and AuNPs when the ATC was added into the solution of UCNPs–AuNPs–AChE mixture, suggesting that AuNPs obviously aggregated. While the parathion-methyl added into the test system, the solution retained in a dispersed state and the solution kept the deep red color (Fig. 2C). Consequently, all these results successfully indicated the sensing principle of the detection of parathion-methyl, which ensures that the quantification of pesticides can be achieved.

3.4. Influence of UCNPs on enzyme activity

It is important and necessary to evaluate the effect of the label-free UCNPs on the enzyme activity. The method for evaluating enzyme activity proposed by Ministry of Health (Determination

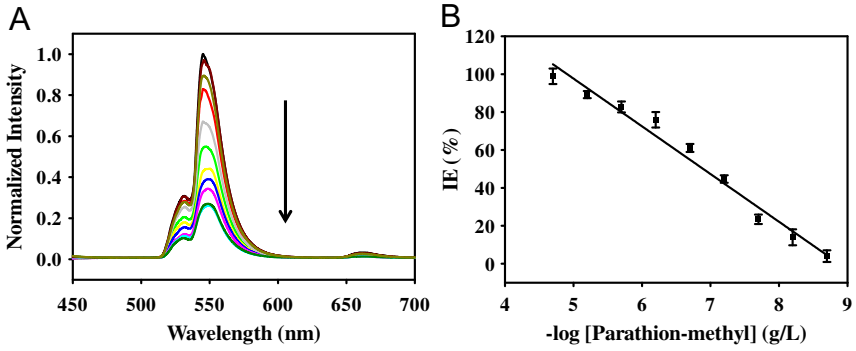

Fig. 3. (A) Fluorescent spectra of UCNPs–AuNPs–AChE-ATC mixed solution with various concentration of parathion-methyl. The concentrations of parathion-methyl (from top to bottom) are 0, 2.0×10^{-9}, 7.0×10^{-9}, 2.0×10^{-8}, 7.0×10^{-8}, 2.0×10^{-7}, 7.0×10^{-7}, 2.0×10^{-6}, 7.0×10^{-6}, and 2.0×10^{-5} g/L, respectively. (B) The linear fitting of the inhibition efficiency vs. concentrations of parathion-methyl.

Standard of the AChE and ChOx, WS/T66-1996) (Kramer and Gamson, 1958) was selected for monitoring the activity of the used enzyme in the presence and absence of UCNPs. Fig. S7 shows the absorbance spectra and color changes of variable concentrations of ACh upon the interaction with AChE, ChOx, and alkaline hydroxylamine. The results have no significant differences in the presence (Fig. S7A and S7C) and absence (Fig. S7B and S7D) of UCNPs, indicating that the UCNPs have no influence on enzyme activity.

3.5. Sensitive detection of pesticides

Fig. 3A displays the fluorescent spectra of UCNPs–AuNPs–AChE in the presence of 10 μM ATC with variable concentrations of parathion-methyl. The fluorescent intensity of UCNPs–AuNPs–AChE-ATC mixture decreased (from top to bottom) with the increase of the parathion-methyl concentration. A good linearity between the inhibition efficiency and the logarithm of the parathion-methyl concentration was observed, ranging from 2×10^{-9} g/L to 2×10^{-5} g/L and a linear regression equation was *IE (inhibition efficiency, %)=25.1714 log[*pesticides*] (g/L)+223.5070* with the correlation coefficient (R^2) of 0.99 as shown in Fig 3B. Where inhibition efficiency was estimated as follows (Yi, et al., 2013):

$$\textit{Inhibition efficiency} = F_{\textit{inhibitor}} - F_{\textit{no inhibitor}}/F_0 - F_{\textit{no inhibitor}} \times 100\% \quad (3)$$

in which $F_{\text{inhibitor}}$ and $F_{\text{no inhibitor}}$ refer to the fluorescence intensities at 550 nm of the UCNPs–AuNPs–AChE-ATC mixture in the presence of different concentrations of parathion-methyl and absence of parathion-methyl, respectively. F_0 refers to the fluorescence intensity of the UCNPs–AuNPs at 550 nm in the absence of AChE and inhibitor. The limit of detection for parathion-methyl was calculated to be 0.67 ng/L ($S/N=3$).

We also analyzed two other conventional pesticides: monocrotophos and dimethoate with the devolved method for demonstrating that the sensing platform was effective not only for parathion-methyl but also for other pesticides. The experimental procedures were the same for the detection of parathion-methyl. As shown in Fig. S10 (A) and (C), the fluorescent intensity of UCNPs–AuNPs–AChE-ATC mixture decreased (from top to bottom) with concentrations of monocrotophos (A) and dimethoate (C). Fig. S10 (B) and (D) shows the relationship between inhibition efficiency and the monocrotophos (B) and dimethoate (D) concentration which exhibited a similar trend to that of parathion-methyl. The detection limit for monocrotophos and dimethoate are 2.3×10^{-8} and 6.7×10^{-6} g/L, respectively, which are much lower than those of the reported methods (Karamfilov et al., 1996; Chauhan and Pundir, 2011; Liang et al., 2012; Yi et al., 2013; Ben Oujji et al., 2014). A comparison between this method and other previously reported methods for pesticides determination is summarized in Table S1.

3.6. Anti-interference capability of the nanosensor

Anti-interference capability is a very important parameter in estimating the performance of a sensor. In order to evaluate the specificity of the biosensor for the detection of pesticide residues, two control experiments were conducted. First, the influences of some potentially common existing substances in food samples, including NaCl, KCl, $FeCl_3$, $MgCl_2$, $AlCl_3$, $CaCl_2$, Na_2SO_4, Na_2CO_3, $ZnCl_2$, Na_3PO_4, $NaHCO_3$, $GdCl_2$, glucose, fructose, 2-nitrophenol, proline, histidine, arginine and vitamin C, were examined. As shown in Fig. 4A, pesticide and other disruptors were mixed together to form a mixture solution as a sample for anti-interference capability testing. The inhibition efficiency of pesticide was identical to that of the mixture of pesticide and other disruptors, which indicated there was no obviously influence. Second, the inhibition efficiency of the UCNPs–AuNPs–ATC-AChE mixed solution in the presence of disruptors of parathion-methyl. The results demonstrated that only parathion-methyl caused significant inhibition efficiencies of the biosensing system (Fig. 4B). And the typical metal ions, organic acids, amine acids and other substances do not exert great interference in parathion-methyl determination. The fluorescent intensity of UCNPs–AuNPs–AChE-ATC mixed solution with various disruptors is shown in Fig. S11. Consequently, all these results have clearly illustrated that the UCNPs based fluorescence biosensor provided excellent specificity and anti-interference capability in pesticide detection.

3.7. Detection of parathion-methyl residues in the food samples

In order to demonstrate the applicability of the developed sensor in complex matrixes, the pesticides in spiked fruit sample such as capsicum, cucumber, and apple were detected. The results obtained by standard addition method was summarized in Table 1. The recoveries in the range from 96.00% to 110.00%. were obtained. The experimental results suggested that this senor has the capability for detection of pesticides in real samples. As we know, pesticides are easily absorbed on the skins of agricultural products and their residues may cause fatal consequences. we also evaluated whether the sensor we described here could be utilized to monitor the residues of pesticides in food samples. The concentration of parathion-methyl residue in capsicum, cucumber, and apple was determined by using the biosensor as shown in Fig. S12 (black). The logarithm of the pesticides concentration had few changes in real samples, indicating that the parathion-methyl residues on the skins of real samples were stable for at least 10 days

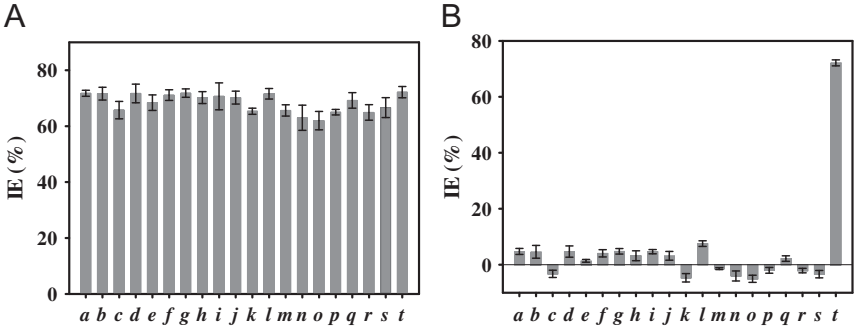

Fig. 4. (A) Effects of possible interference species in analytes (1.0×10^{-3} g/L) on the inhibition efficiency of parathion-methyl (1.0×10^{-6} g/L) in the UCNPs–AuNPs–AChE system. (B) The inhibition efficiency of UCNPs–AuNPs–AChE system mixture with parathion-methyl or other substances. These analytes include NaCl(a), KCl(b), $FeCl_3$(c), $MgCl_2$(d), $AlCl_3$(e), $CaCl_2$(f), Na_2SO_4(g), Na_2CO_3(h), $ZnCl_2$(i), Na_3PO_4(j), $NaHCO_3$(k), $GdCl_2$(l), glucose(m), fructose(n), 2-nitrophenol(o), proline(p), histidine(q), arginine(r), vitamin C(s) and control (t) respectively.

Table 1
Recovery ratios of parathion-methyl in fruit samples.

Sample	Spiked/μg/L	Experimental value (IE %)	Average value/μg/L	Recovery (%)	RSD (%)
Apple	0	8.19			
Apple+parathion	0.030	34.01	0.029	96.67	6.63
Apple+parathion	0.400	63.61	0.440	110.00	7.32
Apple+parathion	3.500	85.90	3.420	97.71	5.57
Capsicum	0	6.96			
Capsicum+parathion	0.030	33.96	0.029	96.67	8.43
Capsicum+parathion	0.400	62.00	0.384	96.00	7.01
Capsicum+parathion	3.50	86.34	3.554	101.54	4.98
Cucumber	0	4.58			
Cucumber+parathion	0.030	34.24	0.032	106.67	6.82
Cucumber+parathion	0.400	62.29	0.394	98.50	4.78
Cucumber+parathion	3.500	86.72	3.572	102.06	5.05

with negligible degradation. From the experimental results, the levels of the parathion-methyl residues on the skins of apple, capsicum and cucumbers were different: the logarithm of the pesticides concentration values for cucumbers were lower than those for apple and capsicum, indicating that parathion-methyl may absorb onto the skins of apple and capsicum more readily than those of cucumbers. In order to further demonstrate the accuracy of this method, the concentration of pesticides in each sample was also analyzed by HPLC according to the literature (Liu et al., 2012; Yi et al., 2013). As shown in Fig. S12 (red), the different parathion-methyl residues in real samples were clearly confirmed by HPLC. The experimental results exhibited that they are consistent with those obtained from the proposed assay, indicating that the proposed method can be used to analyze pesticide residues in real samples accurately. Compared with the HPLC, the assay method of this paper, possess several unique qualities, such as reliable, simple instruments, low cost, easiness for operation, high resistance to photobleaching and photochemical degradation and the assay results can be read as soon as the probe-sample incubation is completed. In particular, low-energy NIR excitation (normally 980 nm) can overcome the interference from background fluorescence and scattered light.

4. Conclusion

In summary, we have successfully developed a novel nanosensor for organophosphorus pesticides detection based on the FRET between the UCNPs and AuNPs. It has been experimentally demonstrated that the label-free UCNPs have no effect on the enzyme activity. The unique feature of this assay method is that pesticides concentration can be analyzed by the fluorescence of UCNPs. And it is found that the inhibitory effect of pesticides on the enzyme activity was linearly dependent on the logarithm of the pesticide concentration. This sensing system has many advantages, such as rapidly, simplicity, highly sensitivity, a wide linear range, high stability and capability of anti-interference. More importantly, sensitive detections of pesticide were obtained by detecting spiked pesticides in complex samples such as foodstuffs. The convenient assay method has provided a promising selection for the rapid screening of pesticide residues in agricultural products and clinic diagnnoses assays.

Acknowledgments

This work was supported by the National Natural Science Foundation of China (21375037, 21275051, 21475043), Scientific Research Fund of Hunan Provincial Science and Technology Department and Education Department (13JJ2020, 12A084), and Doctoral Fund of Ministry of Education of China (No: 20134306110006).

Appendix A. Supplementary material

Supplementary data associated with this article can be found in the online version at http://dx.doi.org/10.1016/j.bios.2014.12.046.

References

Ben Oujji, N., Bakas, I., Istamboulié, G., Ait-Ichou, I., Ait-Addi, E., Rouillon, R., Noguer, T., 2014. Food Control 46, 75–80.
Buonasera, K., D'Orazio, G., Fanali, S., Dugo, P., Mondello, L., 2009. J. Chromatogr. A 1216, 3970–3976.
Chauhan, N., Pundir, C.S., 2011. Anal. Chim. Acta 701, 66–74.
Chen, H.-Q., Xu, J., Yuan, F., Wu, Y., Zhang, Y.-Y., Wang, L., 2013a. Chin. Chem. Lett. 24, 79–81.
Chen, H.-Q., Yuan, F., Wang, L., 2013b. Anal. Methods 5, 2873–2879.
Du, D., Wang, J., Wang, L., Lu, D., Lin, Y., 2011. Anal. Chem. 84, 1380–1385.
Fu, G., Chen, W., Yue, X., Jiang, X., 2013. Talanta 103, 110–115.
Gabaldón, J.A., Maquieira, A., Puchades, R., 2007. Talanta 71, 1001–1010.
Guo, J., Luo, Y., Li, H., Liu, X., Bie, J., Zhang, M., Cao, X., Shen, F., Sun, C., Liu, J., 2013. Anal. Methods 5, 6830–6838.
Ji, X., Song, X., Li, J., Bai, Y., Yang, W., Peng, X., 2007. J. Am. Chem. Soc. 129, 13939–13948.
Jia, L., Pan, J., Zhu, J., 2013. Anal. Methods 5, 5431–5436.
Jiang, X.-X., Shi, H.-Y., Wu, N., Wang, M.-H., 2011. Food Chem. 125, 1385–1389.
Karamfilov, V.K., Fileman, T.W., Evans, K.M., Mantoura, R.F.C., 1996. Anal. Chim. Acta 335, 51–61.
Kramer, D.N., Gamson, R.M., 1958. Anal. Chem. 30, 251–254.
Lee, J., Lee, H.K., 2011. Anal. Chem. 83, 6856–6861.
Li, H., Wang, L., 2013. Analyst 138, 1589–1595.
Li, Z., Wang, Y., Ni, Y., Kokot, S., 2014. Sens. Actuators B 193, 205–211.
Liang, M., Fan, K., Pan, Y., Jiang, H., Wang, F., Yang, D., Lu, D., Feng, J., Zhao, J., Yang, L., Yan, X., 2012. Anal. Chem. 85, 308–312.
Liao, D., Chen, J., Zhou, H., Wang, Y., Li, Y., Yu, C., 2013. Anal. Chem. 85, 2667–2672.
Liu, B., Tan, H., Chen, Y., 2013. Anal. Chim. Acta 761, 178–185.
Liu, C., Wang, Z., Jia, H., Li, Z., 2011. Chem. Commun. 47, 4661–4663.
Liu, D., Chen, W., Wei, J., Li, X., Wang, Z., Jiang, X., 2012. Anal. Chem. 84, 4185–4191.
Liu, G., Lin, Y., 2005. Anal. Chem. 77, 5894–5901.
Ma, C., Bian, T., Yang, S., Liu, C., Zhang, T., Yang, J., Li, Y., Li, J., Yang, R., Tan, W., 2014. Anal. Chem. 86, 6508–6515.
Payá, P., Anastassiades, M., Mack, D., Sigalova, I., Tasdelen, B., Oliva, J., Barba, A., 2007. Anal. Bioanal. Chem. 389, 1697–1714.
Peng, L., Zhang, G., Zhang, D., Xiang, J., Zhao, R., Wang, Y., Zhu, D., 2009. Org. Lett. 11, 4014–4017.
Qian, G., Wang, L., Wu, Y., Zhang, Q., Sun, Q., Liu, Y., Liu, F., 2009. Food Chem. 117, 364–370.
Seebunrueng, K., Santaladchaiyakit, Y., Srijaranai, S., 2014. Chemosphere 103, 51–58.
Tian, Y., Ye, S., Shi, X., Jing, L., Liang, C., Xian, Y., 2011. Analyst 136, 5084–5090.
Viswanathan, S., Radecka, H., Radecki, J., 2009. Biosens. Bioelectron. 24, 2772–2777.
Wang, Y., Wu, Z., Liu, Z., 2012. Anal. Chem. 85, 258–264.
Wu, S., Duan, N., Shi, Z., Fang, C., Wang, Z., 2014. Anal. Chem. 86, 3100–3107.
Yang, Y., Asiri, A.M., Du, D., Lin, Y., 2014. Analyst 139, 3055–3060.
Yi, Y., Zhu, G., Liu, C., Huang, Y., Zhang, Y., Li, H., Zhao, J., Yao, S., 2013. Anal. Chem. 85, 11464–11470.
Yong, D., Liu, C., Yu, D., Dong, S., 2011. Talanta 84, 7–12.
Zhang, K., Mei, Q., Guan, G., Liu, B., Wang, S., Zhang, Z., 2010. Anal. Chem. 82,

9579–9586.
Zhao, J.N., Yi, Y.H., Mi, N.X., Yin, B.D., Wei, M.J., Chen, Q., Li, H.T., Zhang, Y.Y., Yao, S.Z., 2013. Talanta 116, 951–957.
Zhao, Y., Ma, Y., Li, H., Wang, L., 2011. Anal. Chem. 84, 386–395.
Zheng, Z., Li, X., Dai, Z., Liu, S., Tang, Z., 2011a. J. Mater. Chem. 21, 16955–16962.
Zheng, Z., Zhou, Y., Li, X., Liu, S., Tang, Z., 2011b. Biosens. Bioelectron. 26, 3081–3085.
Zhou, L., He, B., Huang, J., Cheng, Z., Xu, X., Wei, C., 2014. ACS Appl. Mater. Interfaces 6, 7719–7727.
Zhu, P., Miao, H., Du, J., Zou, J.-H., Zhang, G.-W., Zhao, Y.-F., Wu, Y.-N., 2014. J. Agric. Food Chem. 62, 7092–7100.